Choice of mother wavelets in CWT spectral decomposition

Satinder Chopra[+] and Kurt J. Marfurt[†]*
[+]Arcis Seismic Solutions, Calgary; [†]The University of Oklahoma, Norman

Summary

Spectral decomposition carried out with the use of the continuous wavelet transform requires the choice of a mother wavelet, which in turn is used to derive a family of wavelet functions. These wavelet functions are scaled and shifted to 'fit' them to the input seismic data traces. Unlike the fixed-length discrete Fourier transform method, the continuous wavelet transform (CWT) window varies with frequency, resulting in better temporal resolution at high frequencies and better frequency resolution. We evaluate the relative value and use of Morlet, Mexican Hat, Derivative of Gaussian (DOG), and the Shannon wavelets in the analysis of a fluvial-deltaic system. Spectral decomposition carried out on two seismic data volumes shows that the Morlet wavelet is more robust and yields better results than the others. While we do not suggest that this conclusion be generalized, we do recommend that this exercise be carried out on a test volume to select the best mother wavelet to be used in the spectral decomposition.

Introduction

Over the last decade or so, spectral decomposition has become a well-established tool that helps in the analysis of subtle stratigraphic plays and fractured reservoirs. As the name suggests, spectral decomposition decomposes the seismic data into individual frequency components that fall within the measured seismic bandwidth, so that the same subsurface geology can be seen at different frequencies. Thin beds or features will be tuned and have relatively higher amplitude at higher frequencies.

Spectral decomposition is carried out by transforming the seismic data from the time domain into the frequency domain. (Partyka et al. (1999) and Marfurt and Kirlin (2001) used a fixed length short window discrete Fourier transform (SWDFT). Since then other methods have been introduced, including the continuous wavelet transform (CWT) (Sinha et al., 2005), the S-transform (Stockwell et al., 1996), or the matching pursuit decomposition (Mallat and Zhang, 1993). Each of these methods have their own applicability and limitations (e.g. Chakaborty and Okaya, 1995; Leppart et al., 2010), and the choice of a particular method often depends on the end objective. For example, the discrete Fourier transform uses an explicit user-defined time window for its computation, and this choice has a bearing on the resolution of the output data. For instance, if the window is defined to be the laterally varying thickness of stratal slices of a picked geologic formation, then the SWDFT will generate cycles/million years vs. cycles per seismic seconds of recording time. The continuous wavelet transform depends on the choice of the mother wavelet, and usually yields higher spectral resolution but reduced temporal resolution. The S-transform method is better than the continuous wavelet transform method, as it yields good temporal and spectral resolution. The matching pursuit method does not need any windowing and also yields good temporal and spectral resolution. However, it is computationally more expensive. There are a number of commercial or proprietary implementations of spectral decomposition that are routinely used in the industry but the first methods are more common.

Continuous Wavelet Transform method

One can compute SWDFT and CWT either by convolving a time domain seismic trace with a kernel function in the time domain, or by multiplying the spectrum of the seismic trace with a suite of filter banks (the Fourier transform of the kernel functions) and converting back to time. In the traditional Fourier Transform method, the kernel is a suite of fixed-length, windowed sines and cosines. The choice of a shorter window results in better temporal resolution at the cost of frequency resolution, and a longer time window results in improved frequency resolution at the cost of temporal resolution.

For the continuous wavelet transform (CWT) method of spectral decomposition, the kernel function is a wavelet that adapts to the frequency of interest. In general, a specific wavelet centered about a given frequency is computed from the mother wavelet by scaling it and shifting. In this manner, the length of the wavelet contains the same number of center (also called peak) frequency cycles. Specifically, if $\boldsymbol{\Psi}(\boldsymbol{\omega})$ is the Fourier transform of the wavelet $\boldsymbol{\Psi}(\boldsymbol{t})$, then the Fourier transform of the same wavelet scaled by say *s*, $\boldsymbol{\Psi}(\frac{\boldsymbol{t}}{\boldsymbol{s}})$ is given as $\boldsymbol{\Psi}(\boldsymbol{s\omega})$.

As the value of *s* increases, the wavelet is compressed, its spectrum dilates and the peak frequency shifts to a higher value. Conversely, as the wavelet is scaled such that it dilates, the value of *s* decreases, its spectrum is compressed and the peak frequency shifts to a lower value. Thus, by varying the scaling factor '*s*', the wavelet family can represent broadband spectra, wherein the spectrum of each wavelet in the family maintains a constant ratio between its peak frequency and the corresponding bandwidth.

Once the mother wavelet is chosen, the CWT of a function at time *u* and scale *s* may be written as

DOI http://dx.doi.org/10.1190/segam2015-5852193.1

$$\boldsymbol{CWT}[\boldsymbol{g}(\boldsymbol{u},\boldsymbol{s})] = \int_{-\delta}^{+\delta} \boldsymbol{g}(\boldsymbol{t}) \frac{\mathbf{1}}{\sqrt{\boldsymbol{s}}} \boldsymbol{\Psi}^{*} \left(\frac{\boldsymbol{t}-\boldsymbol{u}}{\boldsymbol{s}}\right) \boldsymbol{dt} \qquad (1)$$

$$= \boldsymbol{g}(\boldsymbol{u}) * \bar{\boldsymbol{\Psi}}_{\boldsymbol{s}}(\boldsymbol{u}), \qquad (2)$$

where $\bar{\boldsymbol{\Psi}}_{\boldsymbol{s}}(\boldsymbol{t}) = \frac{\mathbf{1}}{\sqrt{\boldsymbol{s}}} \boldsymbol{\Psi}^{*}(-\frac{\boldsymbol{t}}{\boldsymbol{s}})$. (3)

Choice of mother wavelets

Examining the alternative mother wavelets shown in Figure 1 reveals that the Morlet wavelet has side lobes on both sides, the Mexican Hat and DOG wavelet are simple zero phase wavelets, and the Shannon wavelet is a leggy wavelet with a number of side lobes that die out on both sides. These characteristic observations are expected to have a bearing on their suitability and correlation with the seismic signals on which they are applied. One might suspect that the Morlet and Shannon wavelets will have somewhat lower temporal resolution due to their side lobes, in contrast to the Mexican Hat and DOG wavelets which should exhibit higher temporal resolution. Looking at the shape of the Shannon wavelet, one may not know what to expect in terms of spectral decomposition results.

We made use of these four choices as mother wavelets in the CWT method as applied to a number of different seismic data volumes from Alberta, Canada. Here we discuss the results of two of those applications. The first seismic data volume is from south-central Alberta. The target zones are the Mississippian channels that need to be imaged well so that their interpretation can be carried out confidently.

In Figure 2 we show stratal slices from the 30 Hz frequency volumes generated using each of the four above-mentioned wavelets. On the displays, the energy-ratio coherence (Chopra and Marfurt, 2008) is overlaid to aid in the interpretation of the channel boundaries making use of transparency. Notice that the Morlet wavelet 30 Hz frequency stratal slice exhibits a better overall definition of the channels and the point bars as indicated with the magenta and yellow block arrows. The Shannon wavelet as seen in Figure 2d is also close to the Morlet wavelet display seen in Figure 2a.

We generated similar displays at other frequencies and obtained similar results. In Figure 3 we show a comparative display of the spectral magnitude at 40 Hz frequency. Again, notice that the Morlet wavelet display (Figure 3a) exhibits the channel feature better, and the Shannon wavelet is close behind as we saw in Figure 2.

We repeated this exercise on another seismic dataset from the Montney-Dawson area of British Columbia, comprising the Lower to Middle Triassic strata that represent one of the most prolific petroleum systems in Western Canadian Sedimentary Basin. Our focus was on a zone below the Middle Triassic Montney Formation, which is ruptured with two main thrust faults trending in the NW-SE direction.

In Figure 4, we show time slices (t =1768 ms) from the 40 Hz volumes making use of the four mother wavelets under scrutiny. Again, notice the Morlet wavelet display in Figure 4a exhibits the amplitude features as distinct when compared to the equivalent amplitude slice seen in Figure 4e. A quick comparison with the other wavelet displays shows that they are not as clear. The Shannon wavelet display in Figure 4d shows that it is not a close second to the Morlet wavelet displays as we see in Figure 3.

Conclusions

The choice of mother wavelets in the CWT method for spectral decomposition is important. We experimented with four commonly discussed mother wavelets, namely the Morlet, Mexican Hat, DOG and Shannon wavelets in running CWT spectral decomposition on different seismic data volumes and discuss the results of two applications. The mother wavelet which fits the input seismic data by way of better correlation of the family of wavelet functions that are subsequently generated on scaling and shifting, would yield superior results.

Our results show that the Morlet wavelet exhibits more robust results in the CWT approach as compared with the other mother wavelets. As the mother wavelet as well as the derived wavelet functions must adequately adapt to the localized characteristics of the seismic traces and thus would differ from one dataset to another, we infer that the choice of 'best' mother wavelet is data dependent. Thus we do not wish to generalize this conclusion, as it is possible that another mother wavelet may have a better fit with the seismic data and may yield better definition of the events of interest. We however, do wish *to highlight the need to carry out such an exercise* for the spectral decomposition applications that employ the CWT algorithm and require the choice of a mother wavelet.

Acknowledgements

We wish to thank Rongfeng Zhang of Geomodeling Technology Corporation for generating Figure 1 for us. We would also like to thank Arcis Seismic Solutions, TGS, Calgary, Canada for encouraging this work and for permission to present these results.

DOI http://dx.doi.org/10.1190/segam2015-5852193.1

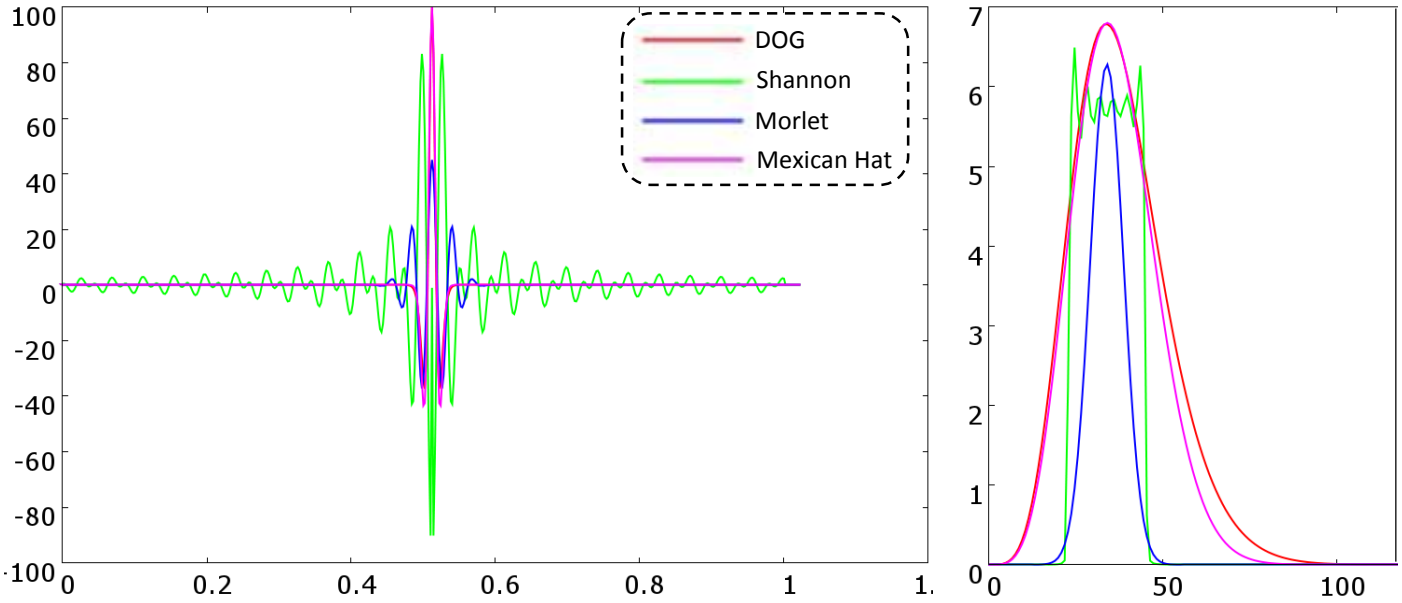

Figure 1: Schematic showing the shapes of Morlet (blue), Mexican Hat (purple), Derivative of Gaussian (DOG)(red), and Shannon (green) wavelets, and their power spectra. All the wavelets have the same center frequency of 35 Hz.

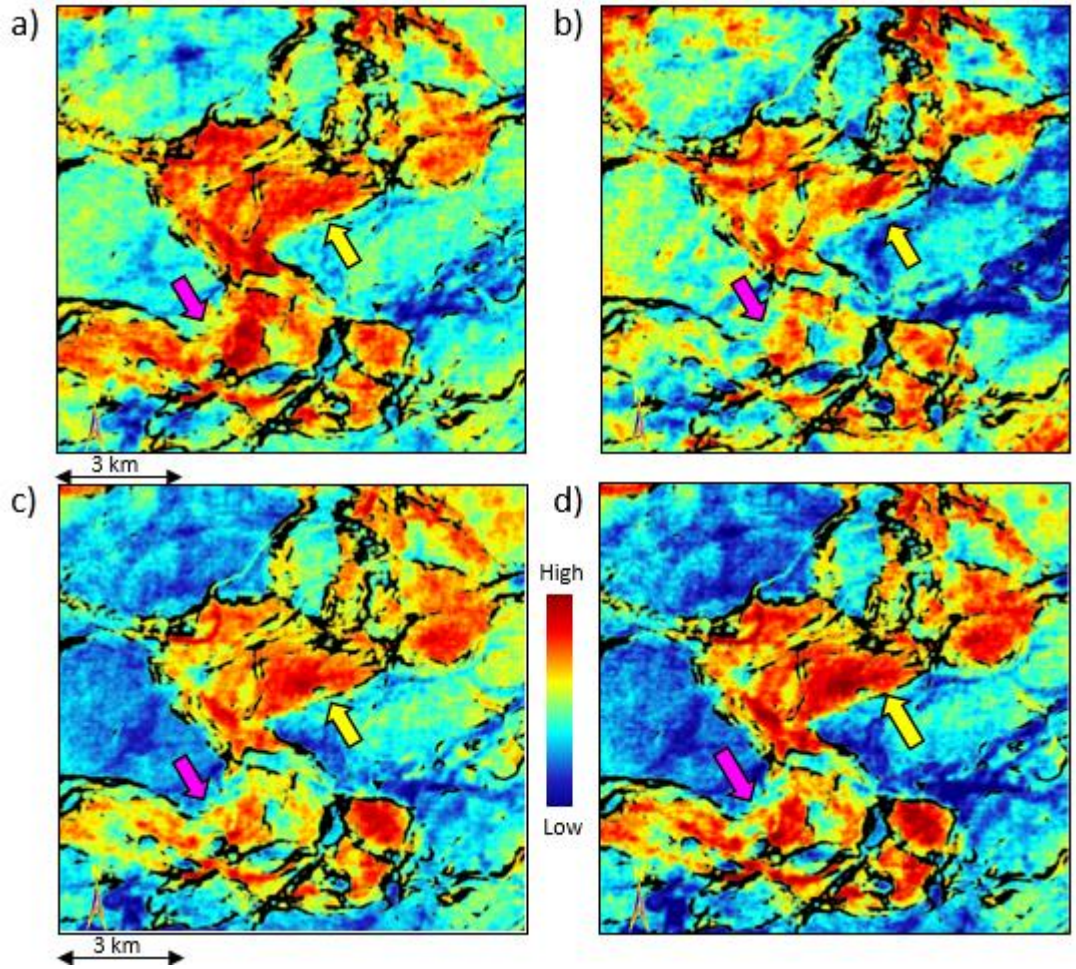

Figure 2: Stratal slices from 30 Hz frequency volumes for a horizon close to 1200ms showing CWT spectral decomposition carried out using (a) Morlet, (b) Mexican Hat, (c) DOG, and (d) Shannon mother wavelets. Overlaid on the displays is the equivalent Energy Ratio coherence attribute with transparency showing only the low coherence values. Notice, the Morlet wavelet display shows the channel features clearly with point bar definitions (indicated with magenta and yellow block arrows) defined well. They are not seen as clearly on the other displays. A close second to the Morlet wavelet display in (a) would be the Shannon wavelet display in (d).
(Data courtesy: Arcis Seismic Solutions, TGS)

DOI http://dx.doi.org/10.1190/segam2015-5852193.1

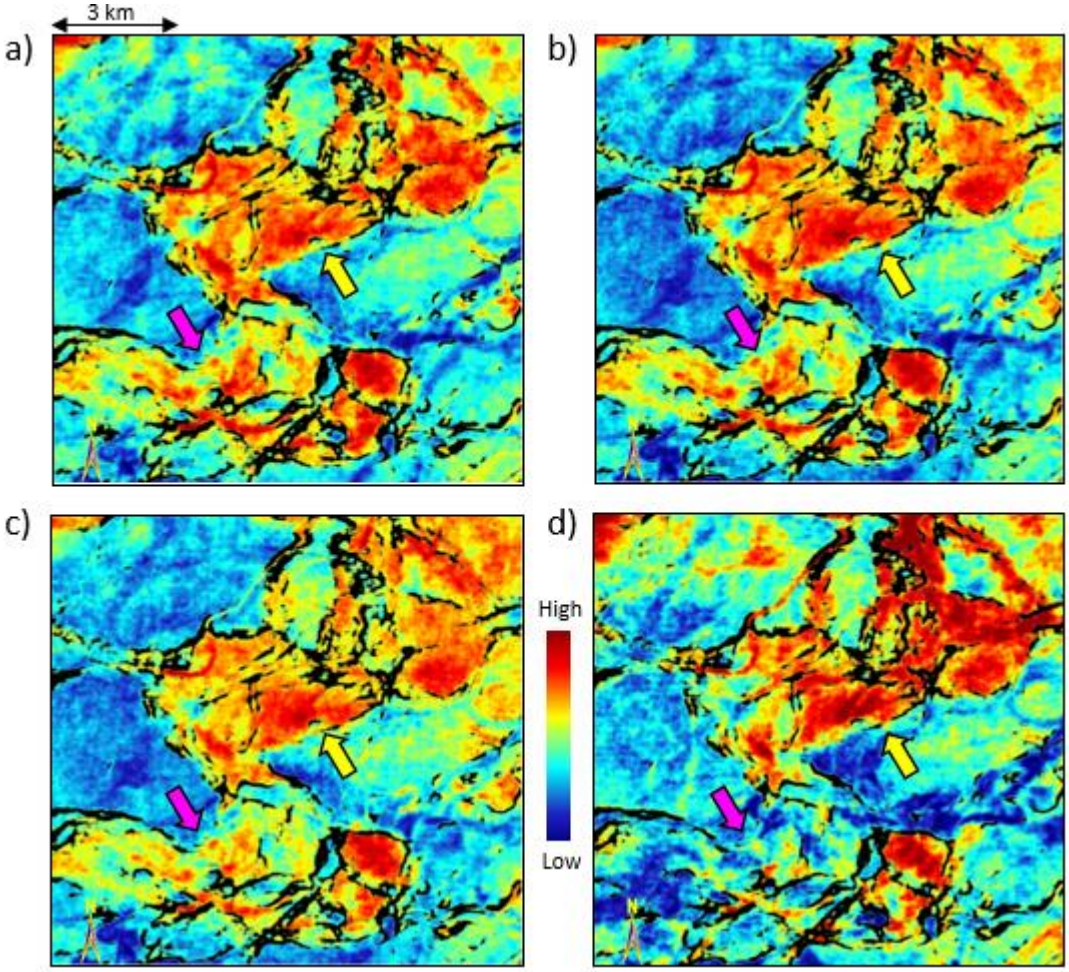

Figure 3: Stratal slices from 40 Hz frequency volumes for a horizon close to 1200ms showing CWT spectral decomposition carried out using (a) Morlet, (b) Mexican Hat, (c) DOG, and (d) Shannon mother wavelets. Overlaid on the displays is the equivalent Energy Ratio coherence attribute with transparency showing only the low coherence values. Notice, the Morlet wavelet display shows the channel features clearly with point bar definitions (indicated with magenta and yellow block arrows) defined well. They are not seen as clearly on the other displays. A close second to the Morlet wavelet display in (a) would be the Shannon wavelet display in (d). *(Data courtesy: Arcis Seismic Solutions, TGS)*

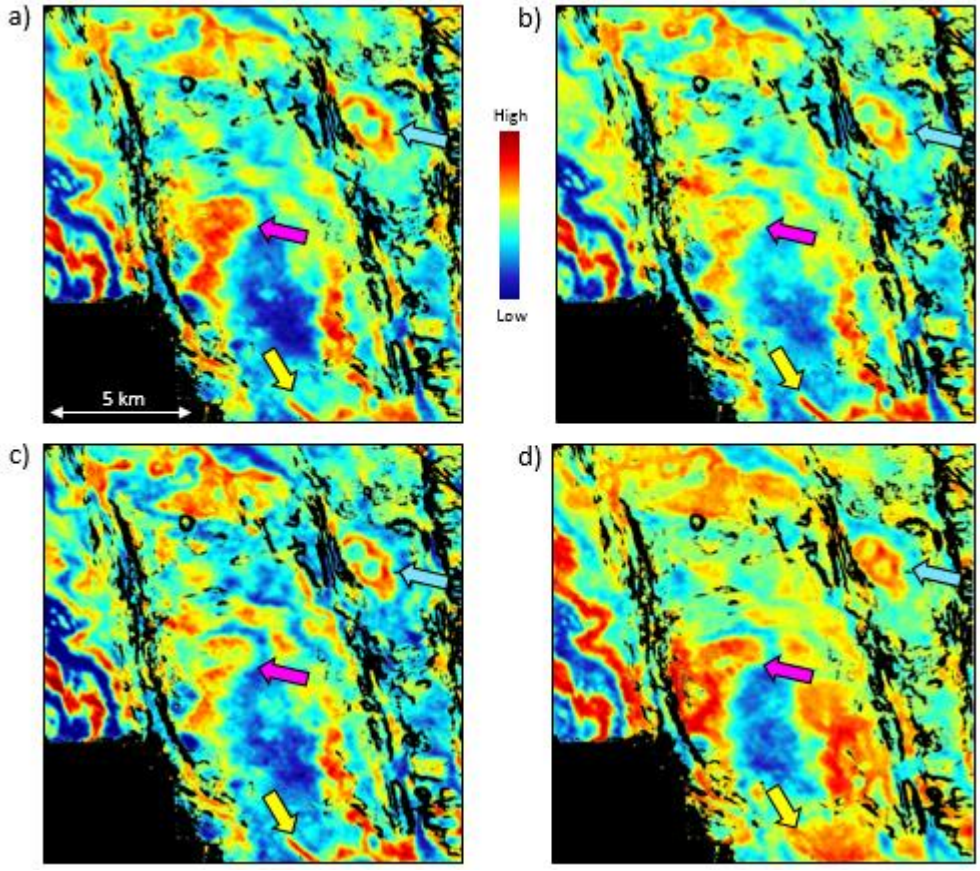

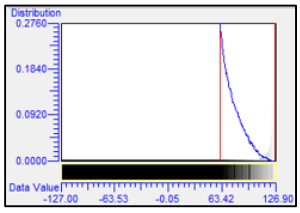

Figure 4: Time slices (1768ms) from 40 Hz volumes showing CWT spectral decomposition carried out using (a) Morlet, (b) Mexican Hat, (c) DOG, and (d) Shannon mother wavelets. Overlaid on the displays is the equivalent Energy Ratio coherence attribute with transparency showing only the low coherence values as per the legend shown above. Notice, the Morlet wavelet display shows some of the features clearly defined as indicated with magenta, yellow and light blue block arrows. They are not seen as clearly on the other displays. On these displays a close second to the Morlet wavelet display in (a) would be the DOG wavelet display in (c), and not the Shannon wavelet display. *(Data courtesy: Arcis Seismic Solutions, TGS).*

DOI http://dx.doi.org/10.1190/segam2015-5852193.1

EDITED REFERENCES

Note: This reference list is a copyedited version of the reference list submitted by the author. Reference lists for the 2015 SEG Technical Program Expanded Abstracts have been copyedited so that references provided with the online metadata for each paper will achieve a high degree of linking to cited sources that appear on the Web.

REFERENCES

Castagna, J. P., and S. Sun, 2006, Comparison of spectral decomposition methods: First Break, **24**, no. 3, 75–79.

Chakraborty, A., and D. Okaya, 1995, Frequency-time decomposition of seismic data using wavelet-based methods: Geophysics, **60**, 1906–1916, http://dx.doi.org/10.1190/1.1443922.

Chopra, S., and K. J. Marfurt, 2008, Gleaning meaningful information from seismic attributes: First Break, **26**, no. 9, 43–53.

Leppard, C., A. Eckersley, and S. Purves, 2010, Quantifying the temporal and spatial extent of depositional and structural elements in 3D seismic data using spectral decomposition and multiattribute RGB blending: Proceedings of the 30th Annual Bob F. Perkins Research Conference, GCSSEPM (Gulf Coast Section of SEPM) Foundation, 1–7.

Mallat, S. G., and Z. Zhang, 1993, Matching pursuits with time-frequency dictionaries: IEEE Transactions on Signal Processing, **41**, no. 12, 3397–3415, http://dx.doi.org/10.1109/78.258082.

Marfurt, K. J., and R. L. Kirlin, 2001, Narrow-band spectral analysis and thin-bed tuning: Geophysics, **66**, 1274–1283, http://dx.doi.org/10.1190/1.1487075.

Partyka, G. A., J. Gridley, and J. Lopez, 1999, Interpretational applications of spectral decomposition in reservoir characterization: The Leading Edge, **18**, 353–360, http://dx.doi.org/10.1190/1.1438295.

Sinha, S., P. S. Routh, P. D. Anno, and J. P. Castagna, 2005, Spectral decomposition of seismic data with continuous-wavelet transform: Geophysics, **70**, no. 6, P19–P25, http://dx.doi.org/10.1190/1.2127113.

Stockwell, R. G., L. Mansinha, and R. P. Lowe, 1996, Localization of the complex spectrum: The S transform: IEEE Transactions on Signal Processing, **44**, no. 4, 998–1001, http://dx.doi.org/10.1109/78.492555.